Injury stimulates stem cells to resist radiation-induced apoptosis

Divya A Shiroor[1], Tisha E Bohr,[1] and Carolyn E Adler[1]*
[1] Department of Molecular Medicine, Cornell University of Veterinary Medicine, 930 Campus Road, Ithaca NY
* Corresponding author – cea88@cornell.edu
(607)-253-3608

Summary
Mechanical injuries cause widespread damage to tissues, fundamentally changing the physiological environment for subsequent repair. How these changes influence stem cells, which are central drivers of tissue repair and regeneration, is unknown. Planarian flatworms are highly capable regenerators, due to an abundant stem cell population that responds to wounding. Injury causes differentiated cells to die (Pellettieri et al., 2010) and stem cells to proliferate (Wenemoser and Reddien, 2010), but how these two events may be linked is unclear. To visualize stem cell dynamics after injury, we reduced their numbers by exposing animals to low doses of radiation (Wagner et al., 2011) and asked how the remaining stem cells respond to damage. We find that stem cells accumulate adjacent to injuries in large numbers, but only if injured within a defined window surrounding radiation. This accumulation occurs despite an absence of proliferation, indicating that stem cells are retained around the wound after radiation. Injury interferes with radiation-induced cell death, as stem cells from injured animals initiate apoptosis at significantly lower rates than uninjured controls. Injury is known to induce apoptosis in differentiated cells. By inducing rampant cell death throughout the body, we find that dying cells are sufficient to prolong survival of radiated stem cells. Together, our results suggest a model in which dying cells provide a protective signal to nearby stem cells, altering their susceptibility to radiation-induced apoptosis.

Results and discussion

Planarians are a highly tractable model system to study regeneration, with a large heterogeneous stem cell population consisting of both pluripotent cells and organ-specific progenitors. (Adler and Sánchez Alvarado, 2015; Newmark and Sánchez Alvarado, 2002; Rink, 2013). When animals are injured, stem cells are recruited to the wound and proliferate to bring about regeneration and repair (Baguñà, 1976; Wenemoser and Reddien, 2010). Previous studies have identified various wound-induced transcriptional changes (Sandmann et al., 2011; Wenemoser and Reddien, 2010; Wurtzel et al., 2015), but how these changes affect stem cell behaviors after injury remain unclear. One impediment is the abundance of this population, which makes it difficult to detect changes in only a few stem cells. We can overcome this problem by exposing animals to radiation, which causes loss of most or all of the stem cells,

depending on the dose. A lethal dose of 6000 rads or higher eliminates all stem cells via apoptosis (Pellettieri et al., 2010), and consequently inhibits regeneration (Bardeen and Baetjer, 1904; Reddien et al., 2005). However, at sublethal doses, some cells survive, eventually repopulating the animal (Lei et al., 2016; Wagner et al., 2011), providing an opportunity to track stem cell behavior after injury. In this study we find that injury promotes stem cell survival by preventing their entry into radiation-induced apoptosis.

Stem cells aggregate adjacent to wounds

To evaluate stem cells, we examined expression of the Argonaute family protein *Smedwi-1*, whose transcript is exclusive to dividing stem cells (Reddien et al., 2005; Scimone et al., 2010). Radiation eliminates stem cells over time. To observe the kinetics of this loss, we first assessed the rate of stem cell depletion after sublethal radiation (2000 rads) by evaluating the expression of *smedwi-1* with quantitative RT-PCR. In accordance with prior studies (Eisenhoffer et al., 2008; Lei et al., 2016), we observed a pronounced decrease in *smedwi-1* 1 day after exposure (Figure 1A). To examine whether this rapid decline impacts the ability of stem cells to respond to injury, we decapitated animals at different times after radiation exposure and monitored stem cell numbers with *in situ* hybridization for *smedwi-1* two days later. Consistent with prior results, decapitation 2-3 days after radiation exposure failed to increase stem cell numbers (Wagner et al., 2011). However, if decapitation occurred within 24 hours of radiation, or immediately after exposure, we observed a significant and pronounced increase in stem cells adjacent to the wound (Figure 1B). This result indicates that stem cells can respond to injury after radiation, but only if the injury occurs within a critical window.

To define the full duration of this response, we reversed the order of radiation and decapitation, and performed amputations prior to radiation exposure. In a mirror image of the sensitivity after radiation, we find that amputations incurred 24 hours prior to radiation also stimulated aggregation of stem cells near the wound (Figure 1C). Therefore, timing of decapitation relative to radiation is crucial. If decapitation occurs 3 days before or after radiation, stem cells fail to respond (Figure 1D). Given the robust and consistent aggregation of stem cells when we decapitated animals within an hour of radiation exposure (n>1000 animals over multiple experiments), we used this paradigm for all further experiments unless otherwise specified.

Our results suggest that injury induces accumulation of stem cells adjacent to the wound site. To examine the dependence of this response on either the position or size of the injury, we varied the location and severity of the wound. Regardless of the type or position of the injury (tail removal or wedges removed pre-pharyngeally), stem cells aggregated adjacent to the wound. In addition, incisions on either side of the head without tissue removal also induced stem cell aggregation (Figure 1E). Together, these data demonstrate that stem cells aggregate locally around any type of injured tissue, but only if the injury occurs within a brief window surrounding the radiation.

To verify that the cells aggregating around the wound were bonafide stem cells, we evaluated other canonical, ubiquitously expressed stem cell transcripts previously identified by transcriptome and expression analyses (Eisenhoffer et al., 2008; Labbé et al., 2012; Solana et

al., 2012). We examined the co-expression of *smedwi-2* together with *smedwi-1* using double fluorescent *in situ* hybridization (FISH) (Reddien et al., 2005; van Wolfswinkel et al., 2014). All *smedwi-1* cells also expressed *smedwi-2*, confirming that cells accumulating around the wound are legitimate stem cells (Supplementary Figure 1A). Other markers of the stem cell population include Histone *H2b* (Solana et al., 2012), the RNA-binding protein *bruli* (Guo et al., 2006), and *soxp-1 (Onal et al., 2012; Wagner et al., 2012; van Wolfswinkel et al., 2014)*. Decapitation induced aggregation of all of these markers adjacent to the wound site (Supplementary Figure 1B), indicating that the phenotypes we observe are not unique to *smedwi-1*.

In addition, planarian stem cells are a heterogeneous population, consisting of both pluripotent stem cells capable of restoring all of the animal's organs (Zeng et al., 2018), and lineage-restricted progenitors. To determine if injury causes persistence of these distinct populations in radiated animals, we examined the expression of *tgs-1* and *zfp-1,* a marker for epidermally-fated stem cells (Tu et al., 2015; van Wolfswinkel et al., 2014). Both of these stem cell markers were present at the wound site (Supplementary Figure 1B), demonstrating that both pluripotent and lineage-restricted progenitor stem cells respond to injury after radiation.

Stem cell persistence is not due to proliferation

Injury in planarians causes stem cells to enter the cell cycle in two waves. A body-wide increase in proliferation occurs 6 hours after any kind of wound, and a second proliferative burst occurs locally 48 hours after tissue removal (Saló and Baguñà, 1984; Wenemoser and Reddien, 2010). Because we observed such a sharp increase in stem cell number after radiation and amputation compared to uninjured controls, we reasoned that proliferation might contribute to this increase. To test this, we stained animals with an antibody recognizing phosphorylated histone H3 at serine10 (H3P) 2 and 7 days after radiation and decapitation. Unirradiated control animals had expected amounts of proliferation at both timepoints. However, we did not detect any proliferating cells in radiated decapitated animals, despite pronounced stem cell aggregation adjacent to the wound (Figure 2A). Therefore, proliferation does not contribute to the stem cell persistence we observe after radiation and decapitation.

If proliferation does not generate new stem cells after injury, an alternative possibility is that stem cells in injured animals are able to resist the effects of radiation. To address this possibility, we visualized early events after radiation by fixing animals at 12 hour intervals after decapitation. At 12 and 24 hours, *smedwi-1* cells were still present throughout the body of decapitated animals. After 24 hours, stem cells in the posterior of the animal diminished strongly (Figure 2B), despite being maintained near the wound for up to 7 days after decapitation (Figure 2C). These data indicate that instead of stimulating proliferation, injury retains radiated stem cells around the wound site. To further test this, we increased the radiation dose from sublethal (2000 rads) to a lethal dose (6000 rads), known to eliminate 100% of stem cells (Eisenhoffer et al., 2008; Reddien et al., 2005; Wagner et al., 2012). We reasoned that if injury induces stem cells to persist, we may still be able to detect them after exposure to a lethal dose of radiation. As expected, 2 days after lethal radiation, intact animals had no stem cells present. By contrast, decapitated animals still had some stem cells around the wound site (Figure 2D and 2E). Injury, therefore, facilitates stem cell persistence after radiation, regardless of the dose.

The prolonged survival of stem cells induced by decapitation suggested that these cells may retain the capacity to differentiate and contribute to regeneration. We therefore examined differentiation with well-established markers of neurons. *Cintillo* and *ovo* are exclusively expressed in small populations of sensory and photoreceptor neurons, respectively (Lapan and Reddien, 2012; Oviedo et al., 2003). Two weeks after radiation exposure and decapitation, we observed partial restoration of both *cintillo* and *ovo* (Supplemental Figure 2A), demonstrating that radiated stem cells are capable of normal differentiation. To determine whether the increased numbers of stem cells we observed could enhance the long-term survival of radiated animals, we exposed animals to sublethal radiation and either left them intact or decapitated them within an hour. Planarians can survive for 2-3 weeks after radiation exposure without continual replenishment from stem cells (Guedelhoefer and Sánchez Alvarado, 2012; Wagner et al., 2011). However, decapitated animals died earlier than uninjured controls (Supplementary Figure 2B), indicating that amputation compromises animal survival. Radiation causes extensive DNA damage and likely impairs the ability of stem cells to sustain the replication demands required to support productive regeneration. Despite the damage caused by radiation, our results demonstrate that stem cells respond to cues in their environment and alter their behavior.

Stem cells resist radiation-induced apoptosis

Exposure to radiation results in a loss of stem cells through radiation-induced apoptosis (Pellettieri et al., 2010). Our results therefore suggest that injury may alter the propensity of radiated stem cells to undergo apoptosis. To test this possibility, we utilized fluorescence-activated cell sorting (FACS), a well-established strategy for isolating a highly enriched population of stem cells (X1) based on DNA content (Hayashi et al., 2006; Reddien et al., 2005). By combining FACS with Annexin V staining, which is routinely used to label apoptosis in intact cells (Crowley et al., 2016), we developed a new method to directly measure cell death in planarian stem cells.

To validate this Annexin V-FACS method in planarians, we first tested whether radiation exposure would increase rates of apoptosis in stem cells. As expected, we observed a precipitous decline in the X1 population from 12.7% in unirradiated animals to 1.6% and 0.66% 1 and 2 days after radiation exposure, respectively (Figure 3A). This decline in the X1 population was accompanied by an increase in the percentage of Annexin V-positive stem cells. Within the stem cell population, we found that in unirradiated controls, only 6% of stem cells were Annexin V-positive, but stem cells from radiated animals displayed significantly higher proportions of X1 cells with increased staining intensity (33.1% and 69.9% 1 and 2 days after radiation) (Figure 3B and 3C). This expected decline in stem cells following radiation, accompanied by an increase in Annexin V staining, confirms that this technique can be used to identify stem cells undergoing apoptosis.

If injury is in fact providing an escape from radiation-induced apoptosis, we predicted that radiated, decapitated animals would have fewer Annexin V-positive stem cells as compared to their intact counterparts. Using Annexin V-FACS, we compared the abundance of apoptotic stem cells in radiated intact and decapitated animals. Consistent with our *in situ* hybridization

results, 1 day after radiation, decapitated animals had more X1 cells as compared to intact animals (7.49% decapitated versus 2.28% intact) (Figure 3D). This population of cells also showed less Annexin V staining than intact animals, both in cell numbers and intensity (32.9% in intact animals versus 10.1% in decapitated animals) (Figure 3E and 3F), indicating that injury interrupts the initiation of apoptosis. Given that we find fewer cells initiating apoptosis in radiated, decapitated animals, we suggest that tissue injury confers resistance to radiation-induced apoptosis.

Death of differentiated cells is sufficient to promote stem cell survival

Studies in *Drosophila*, Hydra and zebrafish have shown that dying cells induce compensatory stem cell proliferation (Brock et al., 2019; Fan and Bergmann, 2008; Huh et al., 2004; Ryoo et al., 2004) and can influence cell survival and fate in a non-autonomous manner (Bilak et al., 2014; Verghese and Su, 2018; Xing et al., 2015). In planarians, injury induces a high concentration of apoptotic cells locally at the wound site (Pellettieri et al., 2010). We combined whole-mount TUNEL (terminal deoxynucleotidyl transferase-mediated dUTP nick end labeling) with *in situ* hybridization for *smedwi-1* to assess the proximity of stem cells to dying cells, and found that they are adjacent, and do not coincide (Figure 4A). Therefore, we considered the possibility that injury-induced apoptosis may also promote stem cell survival.

To directly test whether dying cells may prolong stem cell survival after radiation, we took advantage of previously published pharmacological agents. The translation inhibitor cycloheximide is known to induce apoptosis due to loss of rapidly turned over anti-apoptotic proteins such as Mcl-1 (Adams and Cooper, 2007). Similarly, planarians soaked in cycloheximide exhibit elevated levels of TUNEL staining (Figure 4B) (Pellettieri et al., 2010). To test whether increased apoptosis was sufficient to induce stem cell survival, we soaked animals in cycloheximide for 2 days prior to radiation exposure, and one day afterward. Cycloheximide-soaked animals had markedly increased stem cell numbers after radiation as compared to controls (Figure 4C). We confirmed this effect by measuring *smedwi-1* transcript levels with quantitative RT-PCR (Figure 4D). These results suggest that apoptosis alone, even in the absence of any mechanical injury, is sufficient to prolong stem cell survival after radiation. Because radiation itself induces apoptosis of stem cells, we considered the possibility that these apoptotic stem cells might provide this protective effect to neighboring stem cells. However, we and others have observed massive stem cell loss in radiated, intact animals (Figures 1 and 3). Therefore, we infer that this effect must originate from other cells dying concurrently. Notably, we also observed an increase in stem cell abundance following cycloheximide exposure in unirradiated animals (Figure 4E and 4F). These data imply that dying cells can also regulate stem cell behaviors during homeostasis, even without the added stress of radiation.

Conclusion

The role of apoptosis in planarian homeostasis and regeneration has been mysterious. Ours is the first study to provide evidence that dying cells can influence stem cell behaviour in these animals. Using radiation, which causes stem cells to rapidly initiate apoptosis, we

uncovered a new component of the stem cell response to injury. By pairing injury with radiation, we find that stem cells evade entering apoptosis, but only if the injury occurs within a 'critical period' surrounding radiation. Evidence from other model organisms has shown non-autonomous effects linking apoptotic cells to stem cell behaviors (Chera et al., 2009; Li et al., 2010; Ma et al., 2016; Xing et al., 2015). However, our approach affords a unique perspective because of the acuteness with which the injury is applied, and the direct outcomes on adult stem cells. The pronounced concentration of stem cells around the wound suggests that injury induces local apoptosis, which in turn enables stem cell survival. Our results indicate that apoptosis may impact stem cells both during homeostasis and regeneration, outside the context of radiation. Together, our findings could have broader implications in uncovering cellular behaviours and mechanisms that influence stem cells after routine clinical treatments such as surgery and radiation therapy.

Acknowledgements

We thank Dr. Jason Pellettieri and John Dustin for generously providing us with their optimized TUNEL-FISH protocol; Chris Donahue at the Cornell University Flow Cytometry Core for assistance in optimizing Annexin V staining protocols; Sabrina Solouki and Dr. Avery August for use of their Cell Counter; and Dr. Robert Weiss for maintaining the irradiator. D.A.S. was supported by a GRA Fellowship from the Cornell College of Veterinary Medicine. This work was supported by Cornell University startup funds and a Seed Grant from the Cornell University Stem Cell Program to C.E.A.

Author Contributions

D.A.S. conceived, designed and conducted experiments; analyzed data; wrote the manuscript.
T.E.B. conducted experiments; analyzed data; edited the manuscript.
C.E.A. conceived and designed experiments; wrote the manuscript.

Figure legends:

Figure 1: Injury within a 'critical window' of radiation induces local stem cell persistence.

A) Quantitative RT-PCR of *smedwi-1* relative to GAPDH at specified times after radiation exposure.
B) Animals were exposed to radiation, then decapitated afterwards at indicated times (red).
C) Animals were decapitated at indicated times prior to radiation (red).
D) Magnified images of blastemas from boxed regions in B and C, decapitated at indicated times before or after radiation.
E) Injuries inflicted as indicated in top left corner by red lines. Animals were injured within one hour of radiation exposure. Arrowheads indicate stem cells.

All panels show *smedwi-1 in situ* hybridization in animals fixed 48 hours after injury. Animals were exposed to 2000 rads. Scale bars = 250μm.

Figure 2: Stem cell persistence is not due to proliferation.

A) Phosphohistone H3 (H3P) antibody and *smedwi-1* expression 2 and 7 days after decapitation in unirradiated (top) or radiated (bottom) animals. Dashed boxes highlight zoomed in regions on the right. Scale bars = 100μm.
B) Decapitated animals fixed at indicated timepoints. Boxed regions of *smedwi-1* expression are shown on the right.
C) Quantification of *smedwi-1*$^+$ stem cells in animals 7 days after radiation. Asterisk = $p<0.003$, student's t-test.
D) Animals exposed to lethal radiation (6000 rads) and decapitated within an hour. Red arrows indicate *smedwi-1*$^+$ cells. Second row of images are zoomed regions indicated by box. Scale bar = 250μm.
E) Quantification of *smedwi-1*$^+$ stem cells in D.
For all experiments (except D and E), animals were exposed to 2000 rads.

Figure 3: Stem cells resist radiation-induced apoptosis after injury.

A) FACS plots of Hoechst-stained X1 cells, 1 or 2 days after radiation (dpi). X1 gate is encircled with black lines. Percentage of stem cells within the total population is represented in blue.
B) Histograms of X1 cells from A stained with Annexin V. The percentage of stem cells stained with Annexin V is shown in red. Brackets represent percentage of cells with Annexin V staining above 10^3.
C) Graph of mean fluorescent intensity of Annexin V calculated from bracketed region in B.
D) FACS plots of Hoechst-stained X1 cells. Animals were decapitated within 1 hour of radiation, and processed 24 hours later. X1 gate is encircled with black lines. Percentage of stem cells within the total population is represented in blue.
E) Histograms of X1 cells from D stained with Annexin V. Brackets represent percentage of cells with Annexin V staining above 10^3.
F) Graph of mean fluorescent intensity of Annexin V calculated from bracketed region in D.
Figures representative of N>2 experiments. All X1 cells were isolated from the pre-pharyngeal region 24 hours after exposure to 2000 rads.

Figure 4: Apoptosis promotes stem cell survival.

A) Animals co-stained for TUNEL (magenta) and *smedwi-1 in situ* hybridization (green), 4 hours after radiation and decapitation. Dashed box highlights zoomed regions on the right.
B) TUNEL staining of animals soaked in DMSO (control) or cycloheximide (CHX) for 3 days.
C) *smedwi-1 in situ* hybridization of animals soaked in DMSO or CHX for 2 days prior and 1 day after radiation exposure, then fixed 1 day later.

D) Quantitative RT-PCR of *smedwi-1* relative to GAPDH in animals soaked and radiated as in C. Asterisk represents $p < 0.0014$, Welch's t test.
E) *smedwi-1 in situ* hybridization of animals soaked in DMSO or CHX for 3 days, then fixed 1 day later.
F) Quantitative RT-PCR of *smedwi-1* relative to GAPDH in animals soaked as in E. Asterisk represents $p < 0.003$, Welch's t test.
In A, C, and D, radiation dose was 2000 rads. Scale bars: A,B = 100µm. C = 250µm.

Supplementary Figure 1: Multiple markers of stem cells localize at the wound site.
A) Double fluorescent in situ hybridization of *smedwi-1* (green) and *smedwi-2* (red). Imaged region is highlighted by the box in the cartoon. Percentage represents *smedwi-1*$^+$ cells that co-express *smedwi-2* (white arrowheads). 800 cells were quantified from n=6 animals. Scale bar = 15µm.
B) *in situ* hybridization for stem cell markers as shown. Scale bar = 250µm.
All animals were decapitated within an hour of radiation and fixed 2 days after exposure to 2000 rads. Boxed region is zoomed on the bottom.

Supplementary Figure 2: Radiated stem cells differentiate but do not enhance animal survival.
A) *In situ* hybridization for markers of photoreceptors (*ovo*) and sensory neurons (*cintillo*) at indicated times after decapitation, with and without irradiation. Dashed boxes highlight zoomed regions on the bottom.
B) Kaplan-Meier curves of animal survival of intact (black) and decapitated (red) animals after radiation. n=30 animals.
For all experiments, animals were exposed to 2000 rads.

Materials and Methods

Planarian care and irradiation

Asexual planarians from the *Schmidtea mediterranea* clonal line CIW4 were kept in Montjuïc salts at 20°C (Newmark and Sánchez Alvarado, 2000). Animals used for experiments were between 1-5mm in length and starved for 5-7 days. Planarians were irradiated on a J.L. Shepherd & Associates Mark I-68 Irradiator, and dosage was calculated based on exposure time.

qRT-PCR

A total of 10 animals were processed per biological replicate with 3 biological replicates and 3 technical replicates per condition. Animals were collected in Trizol (Thermo Fisher 15596018) in Lysing Matrix D Tubes (MP Biomedicals 6913100) and homogenized using a Bead Bug microtube homogenizer (Benchmark). RNA was extracted according to the Trizol protocol. cDNA was synthesized using Superscript™ VILO™ (Life Technologies). PCR mixes were made using TaqMan™ Gene Expression Master Mix (Life Technologies). Custom primers are available

at ThermoFisher sequences for *smedwi-1* (AI89MBJ) and GAPDH (AI6RPY3). PCR was run on an Applied Biosystems Viia7 Real Time PCR System and quantified using Ct methods.

Fixations

Animals were fixed and labeled as previously described (Pearson et al., 2009). Briefly, animals were killed using 7.5% N-acetyl-cysteine in PBS for 10 minutes and fixed in 4% paraformaldehyde for 30 minutes at room temperature. After fixation, worms were rinsed twice with PBSTx (PBS + 0.3% Triton X-100). PBSTx was replaced with pre-warmed reduction solution (PBS+ 1% NP-40+ 50mM DTT + 0.5% SDS) and animals were incubated at 37°C for 10 minutes. After rinsing twice with PBSTx, animals were dehydrated in a methanol series and stored at -20°C.

Whole-mount *in situ* hybridizations

Colorimetric *in situ* hybridizations were performed as described in (Pearson et al., 2009) and fluorescent *in situ* hybridizations as in (King and Newmark, 2013) with minor modifications. Briefly, animals fixed as above were rehydrated, bleached (5% Formamide, 1.2% hydrogen peroxide in 0.5x SSC) and treated with proteinase K (4 µg/ml in 1x PBSTx, Thermo Fisher 25530049). Following overnight hybridizations at 56°C, samples were washed 2x each in wash hybe (5 min), 1:1 wash hyb:2X SSC-0.1% Tween 20 (10 min), and 2X SSC (30 min), 0.2X SSC (30 min) at 56°C followed by 3 x 10 minute MABT washes at room temperature. Subsequently, animals were placed in blocking solution (0.5% Roche Western Blocking Reagent and 5% inactivated horse serum diluted in MABT). Animals were then incubated with an appropriate antibody (1:1000 anti-DIG-AP Sigma 1664682, anti-DIG-POD 11207733910 or anti-FITC-POD 11426346910 in blocking solution) at 4°C overnight. Subsequent washes and tyramide development were performed as previously described. After development animals were mounted in ScaleA2 (Hama et al., 2011) (4M urea, 20% glycerol, 0.1% Triton X-100, 2.5% DABCO). Whole-mount *in situ* hybridizations were either imaged on a Leica M165F with a DFC7000T camera or on a Zeiss 710 confocal microscope and images were processed in Fiji (Schindelin et al., 2012). *smedwi-1* stem cells were quantified manually and statistical analysis was carried out using JMP Pro statistical analysis software.

Phosphohistone H3 labeling

Animals were stained with phosphohistone H3 following *in situ* hybridizations. After inactivation of peroxidase with 200mM sodium azide in PBSTx for 1 hour at RT, animals were rinsed in >6 PBSTx washes. Then, animals were incubated in anti-phosphohistone H3 (Ser10) antibody (Abcam, Cambridge, MA Ab32107) at a concentration of 1:1000 in blocking solution for 48 hours at 4°C. Primary was washed off with PBSTx followed by incubation with a goat anti-rabbit-HRP secondary antibody (Thermo Fisher) at a concentration of 1:2000 in PBSTx overnight at 4°C. Antibody was washed off with PBSTx and samples were pre-incubated in fluorescein tyramide (1:5000 in PBSTx) for 10 minutes and then developed with 0.005% H_2O_2 in PBSTx for 10 minutes at room temperature. After development, samples were rinsed in PBSTx and counterstained with DAPI (Thermo Scientific) diluted 1:5000 in PBSTx before mounting in

ScaleA2. Animals were imaged on a Zeiss 710 confocal microscope and images were processed in Fiji (Schindelin et al., 2012).

Flow cytometry and Annexin V staining

Flow cytometry of Hoechst-stained cells was conducted as previously described (Hayashi et al., 2006; Reddien et al., 2005) with minor modifications. Sixty animals per group were placed in 0.065% NAC for 1 minute, followed by rinsing with Montjuïc salt solution. Pre-pharyngeal regions from all animals were dissected and rinsed in CMFB (CMF+0.5% BSA). These fragments were pooled and dissociated using 1:100 Liberase™ (2.5mg/ml, Roche 5401135001) in CMFB at 30°C with gentle agitation at 300 rpm for 30 minutes on a ThermoMixer™ Eppendorf Mixer. Samples were gently triturated every 5 minutes to aid dissociation. Dissociated cells were then diluted with equal volume of CMFB and pelleted by centrifugation (500g, 5 minutes, RT). Pelleted cells were diluted in 1ml of CMFB and strained using a 30µm cell strainer (BD 40627). Strained cells were counted using an automated cell counter (Beckmann Coulter particle counter) and $2.8x10^6$ cells/group were stained with 5µg/ml Hoechst 33342 (ThermoFisher 3H3570) in CFMB for 70 mins in the dark with gentle agitation. Cells were subsequently pelleted and Hoechst solution was replaced with 0.5µl of Annexin V-APC (Thermo Fisher A35110) in 100µl freshly made 1X Annexin V buffer from a 10X stock solution (0.1M Hepes pH 7.4, 1.4M NaCl, and 25 mM $CaCl_2$). After staining for 15 minutes at RT, 400µl of 1X Annexin V buffer with 1µg/ml Propidium Iodide (Sigma P4170-25mg) was added to each tube. Cells were strained again immediately before analysis on a BD FACS AriaII cell sorter. Flow cytometry data was analyzed in FlowJo (TreeStar, Ashland,OR).

TUNEL staining

TUNEL staining protocol was adapted from (Pellettieri et al., 2010). Animals fixed as above were rehydrated and bleached overnight with 6% hydrogen peroxide in PBSTx. Bleached animals were rinsed in PBSTx, permeabilized with Proteinase K (2µg/ml in PBSTx) and post-fixed in 4% formaldehyde for 10 minutes in PBSTx. Animals were rinsed with PBS and transferred to 1.5mL microcentrifuge tubes with a maximum of 5 animals/tube. PBS was replaced with 25µl reaction mix: 3 parts ApopTag TdT enzyme mix, 7 parts ApopTag reaction buffer (Millipore S7107) and incubated overnight at 37°C. Animals were washed with in PBSTx, and blocked for 2 hours (0.5% Roche Western Blocking Reagent and 5% inactivated horse serum in PBSTx) at room temperature. Animals were incubated in antibody (1:1000 anti-DIG-POD in blocking solution) at 4°C for 24 hours. Antibody was washed off with PBSTx and developed using Cy3 tyramide (1:1000 in PBSTx, with 0.005% H2O2) for 10 minutes. After development, samples were counterstained with DAPI (Thermo Scientific) 1:5000 in PBSTx and mounted in ScaleA2, and imaged on a Zeiss 710 confocal microscope. Images were processed in Fiji.

Cycloheximide treatment

Cycloheximide (Sigma 66-81-9) was administered at a concentration of 4µM in planaria water containing a final concentration of 1.5% DMSO. All animals were soaked in cycloheximide for a

total of 72 hours. Unirradiated animals were transferred to planaria water 24 hours prior to fixation. Animals subjected to radiation were soaked 48 hours prior to exposure and maintained in cycloheximide for 24 hours after radiation, then washed and kept in planaria water for another 24 hours before fixing.

TUNEL-FISH

Animals were transferred to 1.5ml eppendorf tubes and incubated in 10% NAC in PBS for 5 minutes, then fixed in 4% paraformaldehyde in PBSTx for 20 minutes at room temperature. After fixation, animals were rinsed twice in PBSTx and permeabilized with proteinase K (20µg/ml) at 37ºC for 10 minutes. Proteinase K was replaced with pre-warmed reduction solution as above and then fixed in 4% paraformaldehyde for 10 minutes. After 2 washes, animals were bleached in 6% H_2O_2 in 100% methanol overnight. Animals were then rinsed in 1X PBS, and 6 animals/tube were incubated in Tdt reaction mix (as above), for 4 hours. Tdt reaction mix was then washed 4x times with PBSTx over 1 hour followed by hybridization with riboprobe as above. The riboprobe was developed using Fluorescein-tyramide as previously described. This was followed by inactivation of peroxidase as above. After washing, animals were incubated overnight at 4ºC with anti-DIG-POD (1:1000) in blocking solution. After washing, TUNEL was developed using Cy3 tyramide as above. Animals were then stained with DAPI, mounted and imaged as above.

REFERENCES

Adams, K.W., and Cooper, G.M. (2007). Rapid turnover of mcl-1 couples translation to cell survival and apoptosis. J. Biol. Chem. *282*, 6192–6200.

Adler, C.E., and Sánchez Alvarado, A. (2015). Types or states? Cellular dynamics and regenerative potential. Trends Cell Biol. *25*, 687–696.

Baguñà, J. (1976). Mitosis in the intact and regenerating planarian *Dugesia mediterranea* n.sp. II. Mitotic studies during regeneration, and a possible mechanism of blastema formation. J. Exp. Zool. *195*, 65–79.

Bardeen, C.R., and Baetjer, F.H. (1904). The inhibitive action of the Roentgen rays on regeneration in planarians. J. Exp. Zool.

Bilak, A., Uyetake, L., and Su, T.T. (2014). Dying cells protect survivors from radiation-induced cell death in Drosophila. PLoS Genet. *10*, e1004220.

Brock, C.K., Wallin, S.T., Ruiz, O.E., Samms, K.M., Mandal, A., Sumner, E.A., and Eisenhoffer, G.T. (2019). Stem cell proliferation is induced by apoptotic bodies from dying cells during epithelial tissue maintenance. Nat. Commun. *10*, 1044.

Chera, S., Ghila, L., Dobretz, K., Wenger, Y., Bauer, C., Buzgariu, W., Martinou, J.-C., and Galliot, B. (2009). Apoptotic cells provide an unexpected source of Wnt3 signaling to drive hydra

head regeneration. Dev. Cell *17*, 279–289.

Crowley, L.C., Marfell, B.J., Scott, A.P., and Waterhouse, N.J. (2016). Quantitation of apoptosis and necrosis by annexin V binding, propidium iodide uptake, and flow cytometry. Cold Spring Harbor Protocols *2016*, db.prot087288.

Eisenhoffer, G.T., Kang, H., and Sánchez Alvarado, A. (2008). Molecular analysis of stem cells and their descendants during cell turnover and regeneration in the planarian *Schmidtea mediterranea*. Cell Stem Cell *3*, 327–339.

Fan, Y., and Bergmann, A. (2008). Apoptosis-induced compensatory proliferation. The Cell is dead. Long live the Cell! Trends Cell Biol. *18*, 467–473.

Guedelhoefer, O.C., 4th, and Sánchez Alvarado, A. (2012). Amputation induces stem cell mobilization to sites of injury during planarian regeneration. Development *139*, 3510–3520.

Guo, T., Peters, A.H.F.M., and Newmark, P.A. (2006). A Bruno-like gene is required for stem cell maintenance in planarians. Dev. Cell *11*, 159–169.

Hama, H., Kurokawa, H., Kawano, H., Ando, R., Shimogori, T., Noda, H., Fukami, K., Sakaue-Sawano, A., and Miyawaki, A. (2011). Scale: a chemical approach for fluorescence imaging and reconstruction of transparent mouse brain. Nat. Neurosci. *14*, 1481–1488.

Hayashi, T., Asami, M., Higuchi, S., Shibata, N., and Agata, K. (2006). Isolation of planarian X-ray-sensitive stem cells by fluorescence-activated cell sorting. Dev. Growth Differ. *48*, 371–380.

Huh, J.R., Guo, M., and Hay, B.A. (2004). Compensatory proliferation induced by cell death in the Drosophila wing disc requires activity of the apical cell death caspase Dronc in a nonapoptotic role. Curr. Biol. *14*, 1262–1266.

King, R.S., and Newmark, P.A. (2013). In situ hybridization protocol for enhanced detection of gene expression in the planarian *Schmidtea mediterranea*. BMC Dev. Biol. *13*.

Labbé, R.M., Irimia, M., Currie, K.W., Lin, A., Zhu, S.J., Brown, D.D.R., Ross, E.J., Voisin, V., Bader, G.D., Blencowe, B.J., et al. (2012). A Comparative Transcriptomic Analysis Reveals Conserved Features of Stem Cell Pluripotency in Planarians and Mammals. Stem Cells *30*, 1734–1745.

Lapan, S.W., and Reddien, P.W. (2012). Transcriptome analysis of the planarian eye identifies *ovo* as a specific regulator of eye regeneration. Cell Rep. *2*, 294–307.

Lei, K., Thi-Kim Vu, H., Mohan, R.D., McKinney, S.A., Seidel, C.W., Alexander, R., Gotting, K., Workman, J.L., and Sánchez Alvarado, A. (2016). Egf Signaling Directs Neoblast Repopulation by Regulating Asymmetric Cell Division in Planarians. Dev. Cell *38*, 413–429.

Li, F., Huang, Q., Chen, J., Peng, Y., Roop, D.R., Bedford, J.S., and Li, C.-Y. (2010). Apoptotic cells activate the “phoenix rising” pathway to promote wound healing and tissue regeneration. Sci. Signal. *3*, ra13.

Ma, M., Zhao, H., Zhao, H., Binari, R., Perrimon, N., and Li, Z. (2016). Wildtype adult stem cells,

unlike tumor cells, are resistant to cellular damages in Drosophila. Dev. Biol. *411*, 207–216.

Newmark, P.A., and Sánchez Alvarado, A. (2000). Bromodeoxyuridine specifically labels the regenerative stem cells of planarians. Dev. Biol. *220*, 142–153.

Newmark, P.A., and Sánchez Alvarado, A. (2002). Not your father's planarian: a classic model enters the era of functional genomics. Nat. Rev. Genet. *3*, 210–219.

Onal, P., Grün, D., Adamidi, C., Rybak, A., Solana, J., Mastrobuoni, G., Wang, Y., Rahn, H.-P., Chen, W., Kempa, S., et al. (2012). Gene expression of pluripotency determinants is conserved between mammalian and planarian stem cells. EMBO J. *31*, 2755–2769.

Oviedo, N.J., Newmark, P.A., and Sánchez Alvarado, A. (2003). Allometric scaling and proportion regulation in the freshwater planarian *Schmidtea mediterranea*. Dev. Dyn. *226*, 326–333.

Pearson, B.J., Eisenhoffer, G.T., Gurley, K.A., Rink, J.C., Miller, D.E., and Sánchez Alvarado, A. (2009). Formaldehyde-based whole-mount in situ hybridization method for planarians. Dev. Dyn. *238*, 443–450.

Pellettieri, J., Fitzgerald, P., Watanabe, S., Mancuso, J., Green, D.R., and Sánchez Alvarado, A. (2010). Cell death and tissue remodeling in planarian regeneration. Dev. Biol. *338*, 76–85.

Reddien, P.W., Oviedo, N.J., Jennings, J.R., Jenkin, J.C., and Sánchez Alvarado, A. (2005). SMEDWI-2 is a PIWI-like protein that regulates planarian stem cells. Science *310*, 1327–1330.

Rink, J.C. (2013). Stem cell systems and regeneration in planaria. Dev. Genes Evol. *223*, 67–84.

Ryoo, H.D., Gorenc, T., and Steller, H. (2004). Apoptotic cells can induce compensatory cell proliferation through the JNK and the Wingless signaling pathways. Dev. Cell *7*, 491–501.

Saló, E., and Baguñà, J. (1984). Regeneration and pattern formation in planarians. I. The pattern of mitosis in anterior and posterior regeneration in Dugesia (G) tigrina, and a new proposal for blastema formation. J. Embryol. Exp. Morphol. *83*, 63–80.

Sandmann, T., Vogg, M.C., Owlarn, S., Boutros, M., and Bartscherer, K. (2011). The head-regeneration transcriptome of the planarian Schmidtea mediterranea. Genome Biol. *12*, R76.

Schindelin, J., Arganda-Carreras, I., Frise, E., Kaynig, V., Longair, M., Pietzsch, T., Preibisch, S., Rueden, C., Saalfeld, S., Schmid, B., et al. (2012). Fiji: an open-source platform for biological-image analysis. Nat. Methods *9*, 676–682.

Scimone, M.L., Meisel, J., and Reddien, P.W. (2010). The Mi-2-like Smed-CHD4 gene is required for stem cell differentiation in the planarian *Schmidtea mediterranea*. Development *137*, 1231–1241.

Solana, J., Kao, D., Mihaylova, Y., Jaber-Hijazi, F., Malla, S., Wilson, R., and Aboobaker, A. (2012). Defining the molecular profile of planarian pluripotent stem cells using a combinatorial

RNAseq, RNA interference and irradiation approach. Genome Biol. *13*, R19.

Tu, K.C., Cheng, L.-C., T K Vu, H., Lange, J.J., McKinney, S.A., Seidel, C.W., and Sánchez Alvarado, A. (2015). Egr-5 is a post-mitotic regulator of planarian epidermal differentiation. eLife *4*, e10501.

Verghese, S., and Su, T.T. (2018). Ionizing radiation induces stem cell-like properties in a caspase-dependent manner in Drosophila. PLoS Genet. *14*, e1007659.

Wagner, D.E., Wang, I.E., and Reddien, P.W. (2011). Clonogenic neoblasts are pluripotent adult stem cells that underlie planarian regeneration. Science *332*, 811–816.

Wagner, D.E., Ho, J.J., and Reddien, P.W. (2012). Genetic regulators of a pluripotent adult stem cell system in planarians identified by RNAi and clonal analysis. Cell Stem Cell *10*, 299–311.

Wenemoser, D., and Reddien, P.W. (2010). Planarian regeneration involves distinct stem cell responses to wounds and tissue absence. Dev. Biol. *344*, 979–991.

van Wolfswinkel, J.C., Wagner, D.E., and Reddien, P.W. (2014). Single-cell analysis reveals functionally distinct classes within the planarian stem cell compartment. Cell Stem Cell *15*, 326–339.

Wurtzel, O., Cote, L.E., Poirier, A., Satija, R., Regev, A., and Reddien, P.W. (2015). A generic and cell-type-specific wound response precedes regeneration in planarians. Dev. Cell *35*, 632–645.

Xing, Y., Su, T.T., and Ruohola-Baker, H. (2015). Tie-mediated signal from apoptotic cells protects stem cells in Drosophila melanogaster. Nat. Commun. *6*, 7058.

Zeng, A., Li, H., Guo, L., Gao, X., McKinney, S., Wang, Y., Yu, Z., Park, J., Semerad, C., Ross, E., et al. (2018). Prospectively Isolated Tetraspanin+ Neoblasts Are Adult Pluripotent Stem Cells Underlying Planaria Regeneration. Cell *173*, 1593–1608.e20.

Figure 1: Injury within a 'critical window' of radiation induces local stem cell persistence.

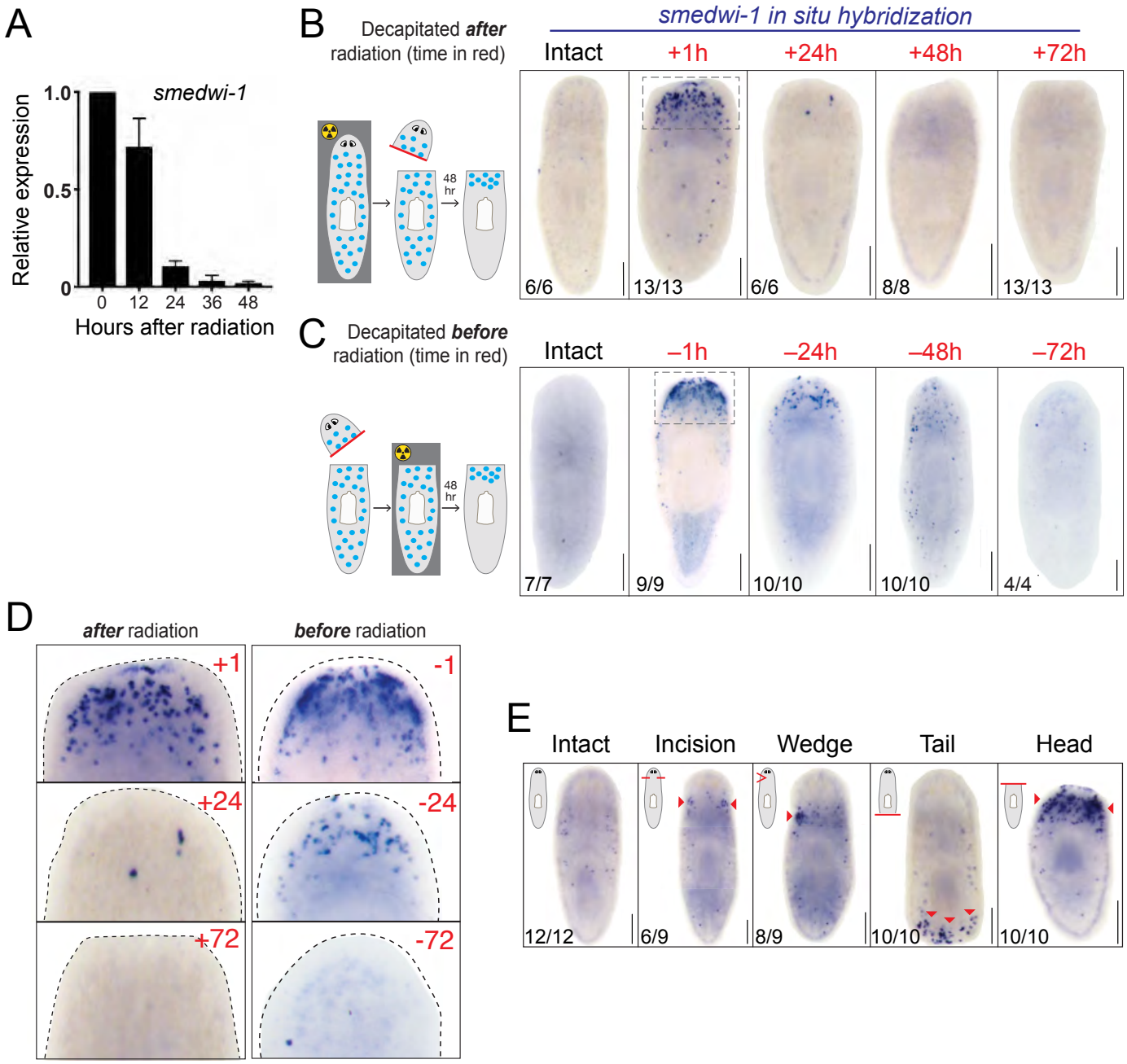

Figure 2: Stem cell persistence is not due to proliferation.

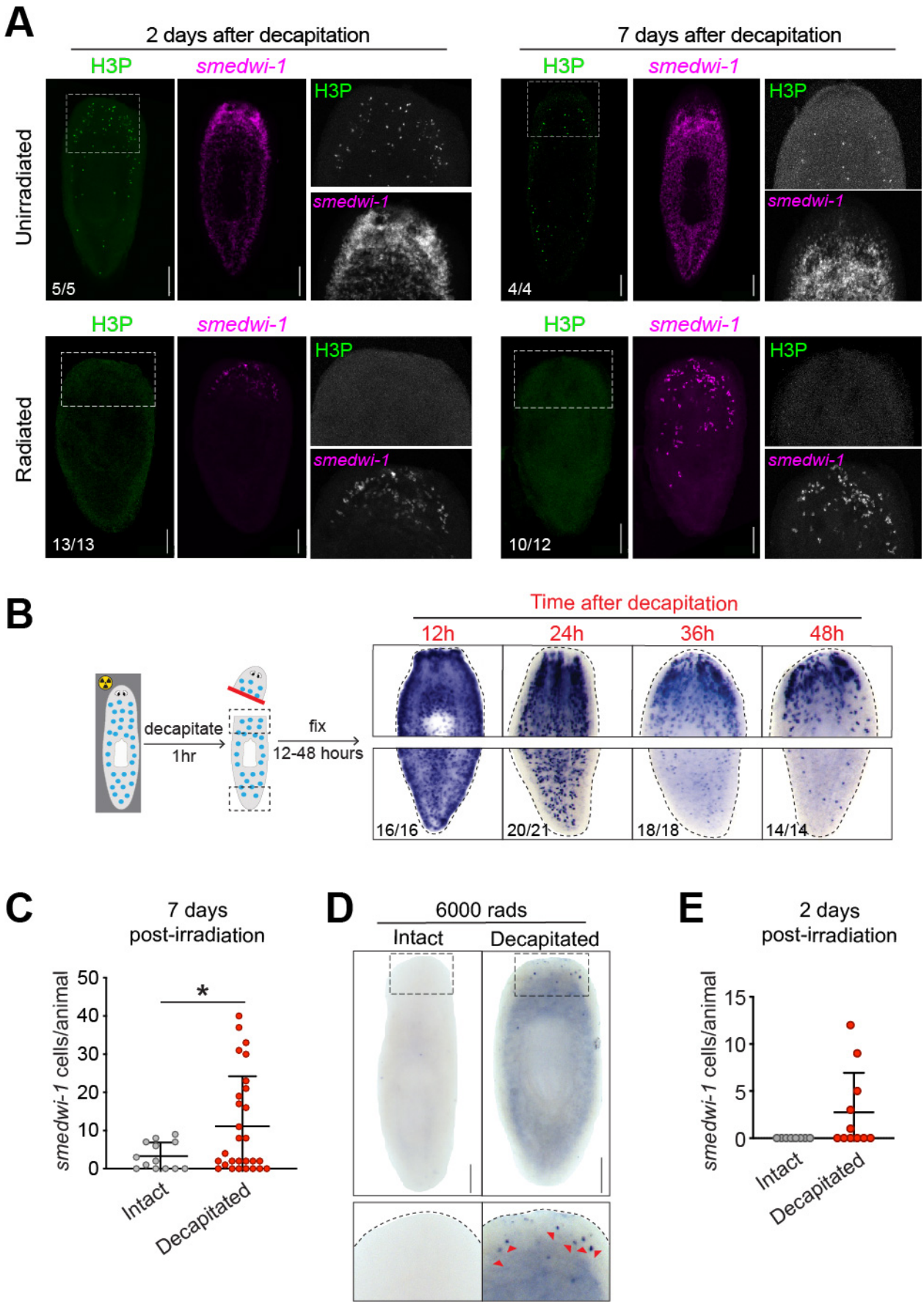

Figure 3: Stem cells resist radiation-induced apoptosis after injury.

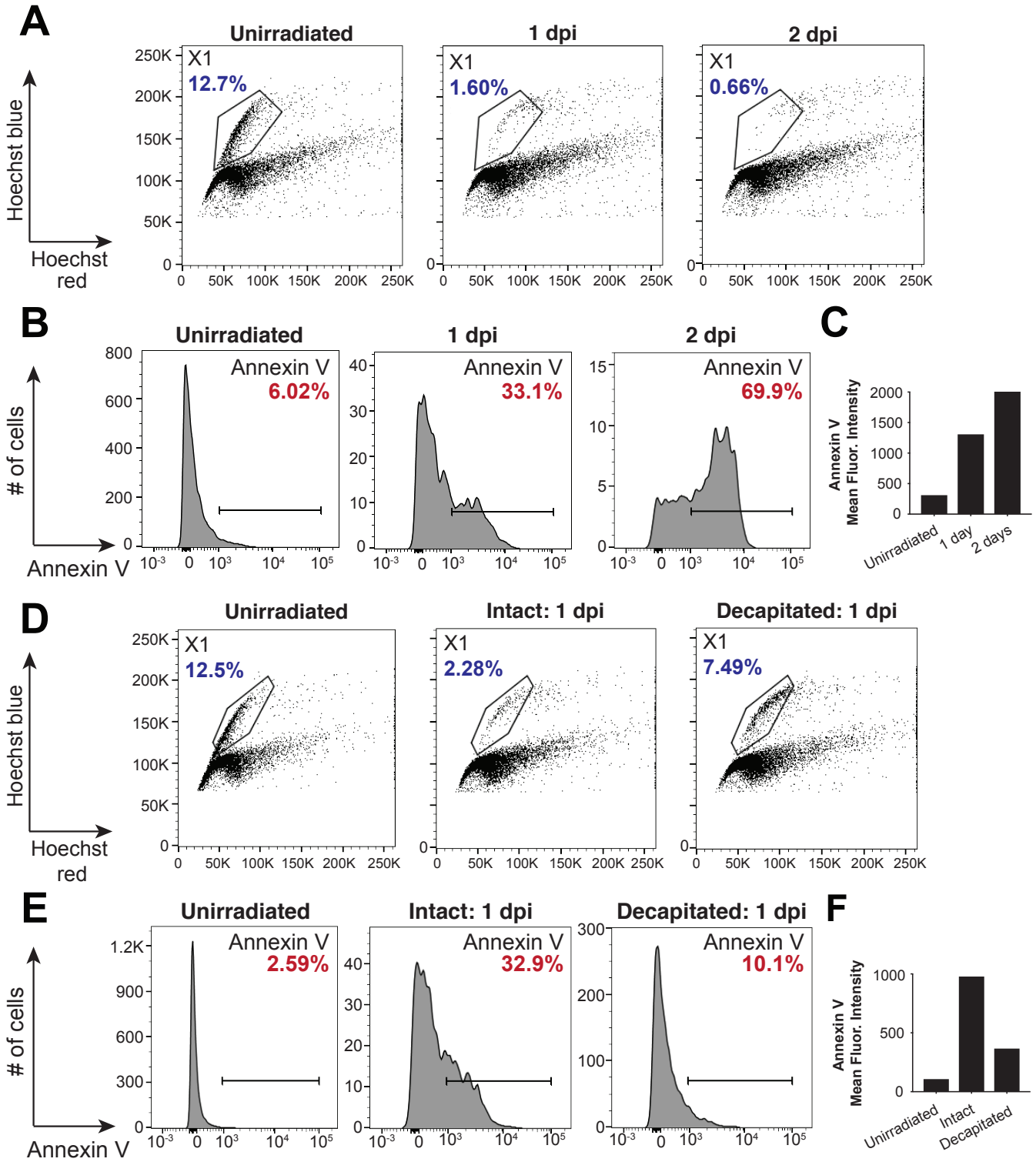

Figure 4: Apoptosis promotes stem cell survival.

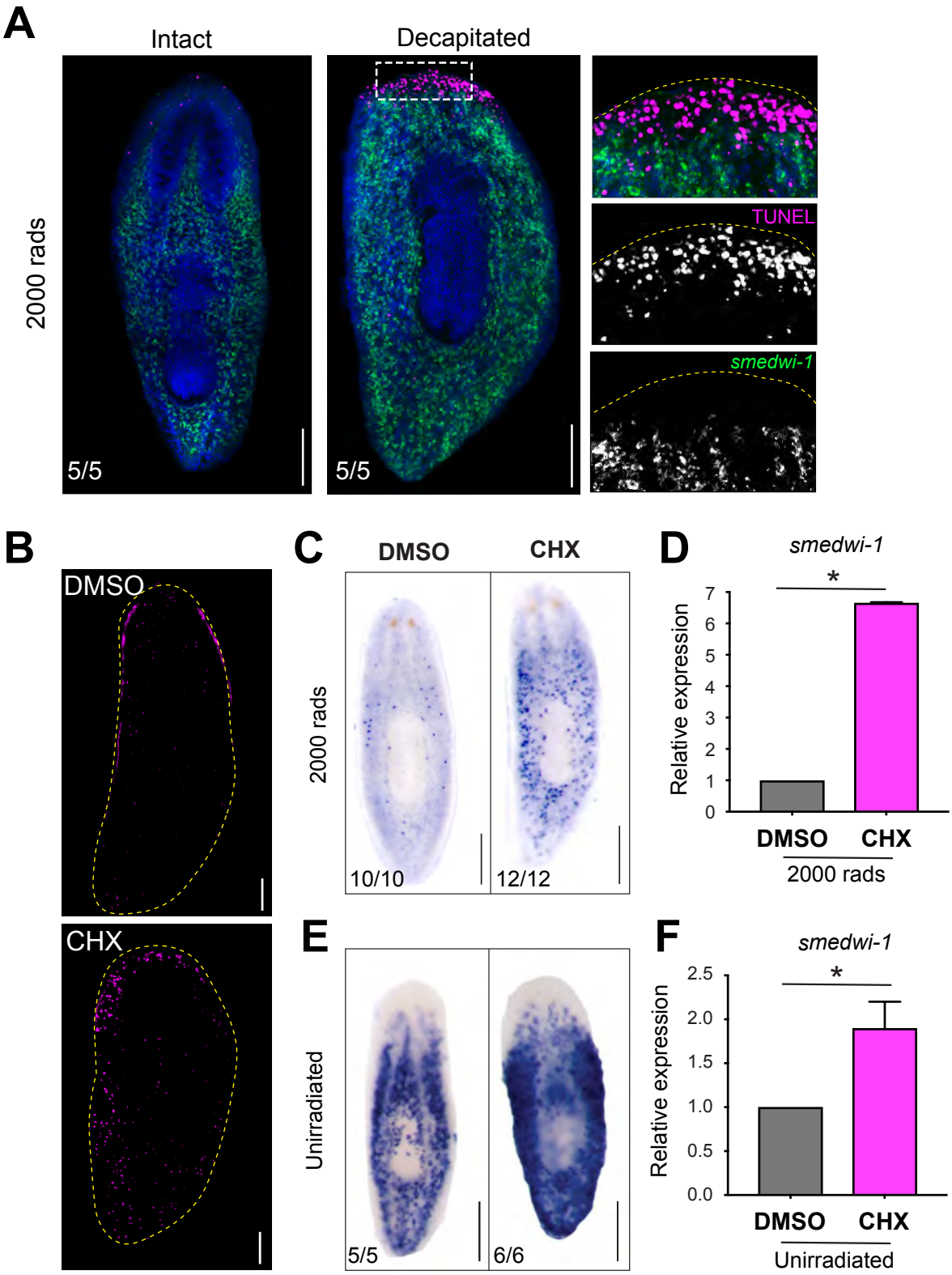

Supplementary Figure 1: Multiple markers of stem cells localize at the wound site.

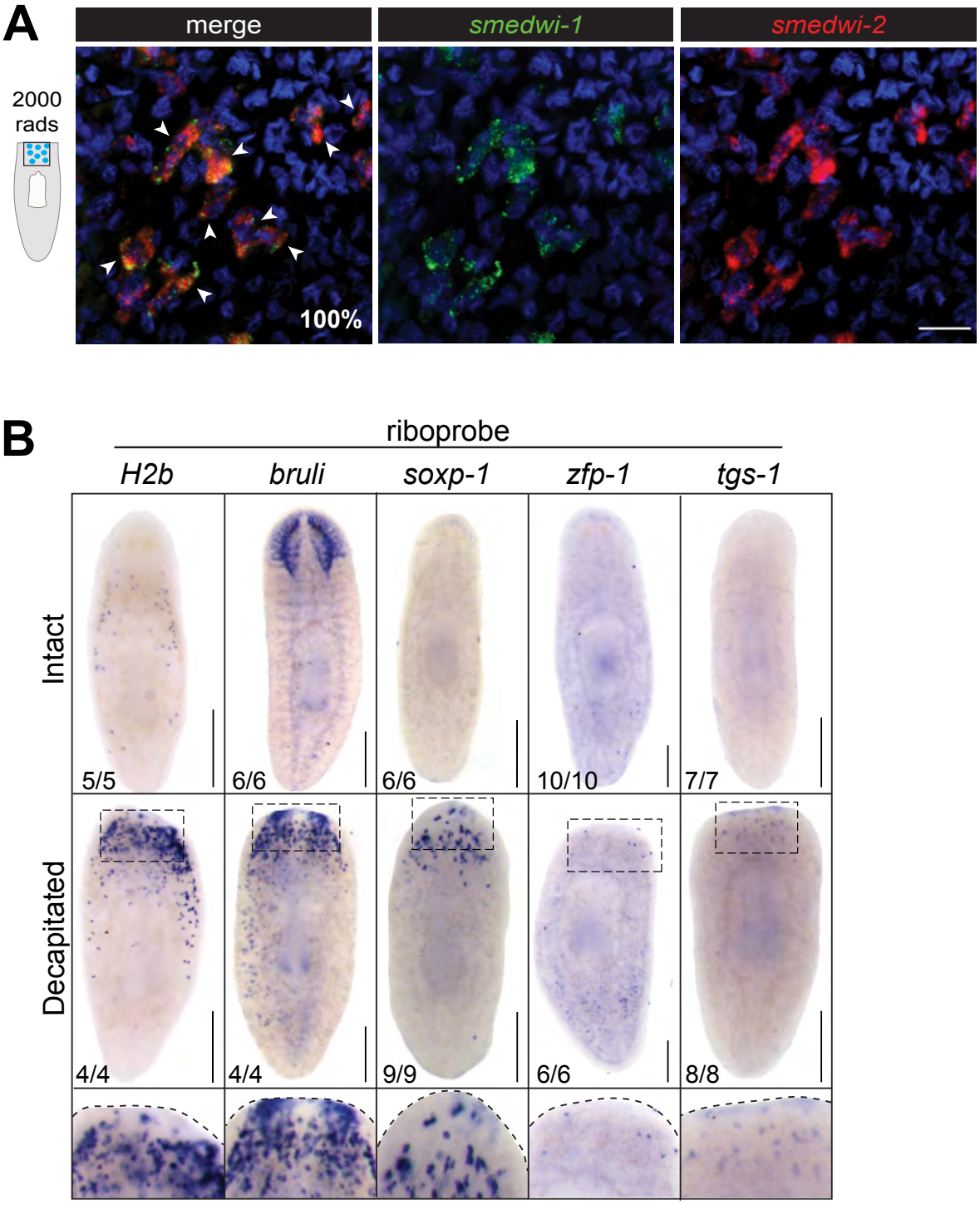
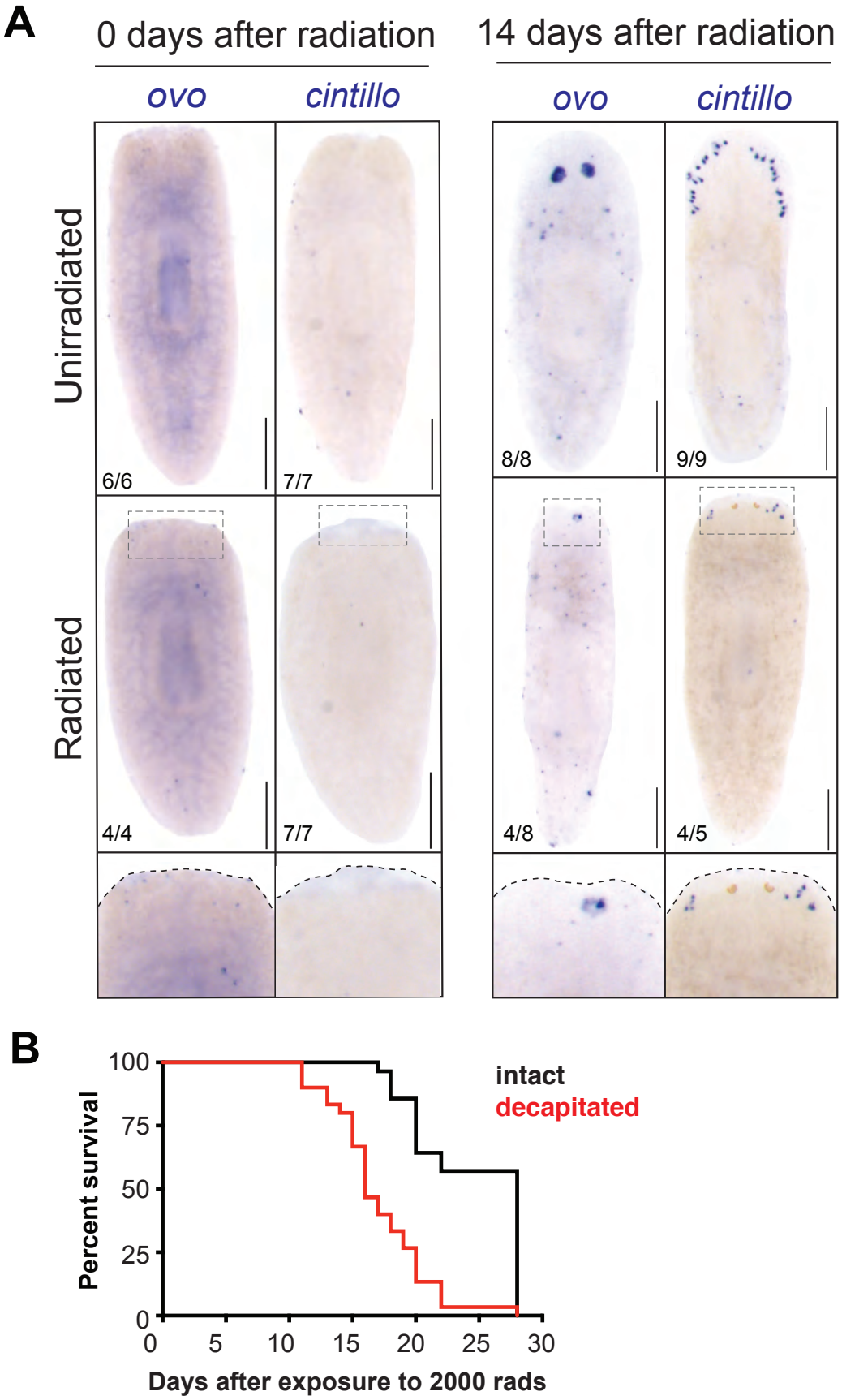
Supplementary Figure 2: Radiated stem cells differentiate but do not enhance animal survival.